Role of Crystalline Defects in Electrocatalysis: Mechanism and Kinetics of CO Adlayer Oxidation on Stepped Platinum Electrodes

N. P. Lebedeva,*,† M. T. M. Koper,† J. M. Feliu,‡ and R. A. van Santen†

Schuit Institute of Catalysis, Laboratory of Inorganic Chemistry and Catalysis, Eindhoven University of Technology, 5600 MB Eindhoven, The Netherlands, and Departamento de Quimica Fisica, Universidad de Alicante, Apartado 99, E-03080 Alicante, Spain

Received: February 12, 2002

The kinetics of the electrochemical oxidation of a CO adlayer on Pt[*n*(111)×(111)] electrodes in 0.5 M H_2SO_4 has been studied using chronoamperometry. The objective is to elucidate the effect of the crystalline defects on the rate of the reaction by using a series of stepped surfaces. The reaction kinetics of the main oxidative process can be modeled using the mean-field approximation for the Langmuir−Hinshelwood mechanism, implying fast diffusion of adsorbed CO on the Pt[*n*(111)×(111)] surfaces under electrochemical conditions. The apparent rate constant for the electrochemical CO oxidation, determined by a fitting of the experimental data with the mean-field model, is found to be proportional to the step fraction (1/n) for the surfaces with $n > 5$, proving steps to be the active sites for the CO adlayer oxidation. An apparent intrinsic rate constant is determined. The potential dependence of the apparent rate constants is found to be structure insensitive with a Tafel slope of ca. 80 mV/dec, suggesting the presence of a slow chemical step in an ECE reaction mechanism.

1. Introduction

Many surface chemical reactions are known to be "structure-sensitive".[1,2] For mechanistic studies it is therefore especially important to perform experiments on well-defined single-crystal surfaces. These model surfaces can also be designed to expose varying densities and structures of atomic steps and/or kinks, thus allowing the systematic investigation of the influence of surface defects on the reaction kinetics and mechanism.[1]

At steps and kinks atoms have a lower coordination and are generally more reactive than atoms on a flat surface.[2−4] A main reason for the enhanced activity of defects is the altered electronic structure at such sites, since the local *d* band narrows and shifts upward in energy closer to the Fermi level.[4,5] This results in a higher adsorption energy for many molecular and atomic adsorbates on step and kink sites (for example, carbon monoxide,[3,4,6] molecular and atomic oxygen,[7] nitric oxide, atomic and molecular nitrogen[8]). As a consequence, and in accordance with the Bronsted−Polanyi relation,[9] lower activation energies for molecular dissociation reactions are often observed at step and kink sites,[7,8] and these low-barrier reaction paths were found to totally dominate the reactivity in some cases.[8b,8d] However, in a recent study, steps were found to be the active sites in oxygen dissociation on Pt without providing the lowest activation barrier.[10] The enhanced reactivity in this case might be related to a preferential adsorption of the reactant on the steps.

In electrocatalysis steps and kinks are also known to be more reactive than flat surfaces. For example, a preferential adsorption of CO on both (100) and (110) steps on platinum has been observed at low CO coverages,[11,12] and also the oxidation of water in sulfuric acid solution on platinum is facilitated by all kinds of crystalline defects.[13] Steps of (110) orientation and crystalline defects were shown to catalyze CO oxidation on Pt[12,14,15−17] and Rh.[18] It has also been found that the dehydrogenation of formic acid is favored at both (100) and (110) steps, but since CO formed adsorbs strongly at the steps the steady-state reactivity is low.[19] The same holds for the electrochemical ethylene glycol[20] and ethanol[21] oxidation. Despite the significant amount of qualitative evidence for the enhanced activity of step and kink sites in various electrochemical reactions, a more quantitative understanding of their role in electrocatalysis has been less forthcoming. Our goal in this paper is to establish a quantitative link between step fraction and the kinetics of an important model reaction in electrocatalysis, the electooxidation of adsorbed CO.

The electrochemical oxidation of CO on platinum is certainly among the most extensively studied reactions over the past decades, since it is of both fundamental and practical interest. The achievements until 1990 in the understanding of this reaction have been reviewed by Beden et al.[22]

The "reactant-pair" mechanism for the electrochemical oxidation of adsorbed CO in acidic solutions, originally proposed by Gilman,[23] is now generally accepted. This mechanism assumes a Langmuir−Hinshelwood type reaction between carbon monoxide and a surface oxygen-containing species, adsorbed on adjacent sites, to form CO_2. The oxygen-containing species results from the oxidation of water at the electrode surface and is usually supposed to be OH_{ads}, although the exact nature of this species is still elusive. Since the potential dependence of the reaction was found to be about 70−80 mV/dec, the presence of a slow chemical step in the reaction scheme was suggested in a number of publications.[15,24] The overall reaction scheme is

$$H_2O + * \rightleftarrows OH_{ads} + H^+ + e^- \quad (1)$$

$$CO_{ads} + OH_{ads} \rightarrow COOH_{ads} \quad (2)$$

$$COOH_{ads} \rightarrow CO_2 + H^+ + e^- + 2* \quad (3)$$

* Corresponding author. Present address: Energieonderzoek Centrum Nederland, unit Schoon Fossiel, Postbus 1, 1755 ZG Petten, The Netherlands. Tel.: +31-224-564408. Fax: +31-224-568489. E-mail: lebedeva@ecn.nl.

† Eindhoven University of Technology.

‡ Universidad de Alicante.

10.1021/jp0204105 CCC: $22.00 © 2002 American Chemical Society
Published on Web 11/27/2002

where "*" denotes a free surface site, reactions 1 and 3 are fast, and reaction 2 is the rate-determining step (at least at relatively high overpotentials as studied in this work).

The rate of reaction 2 depends markedly on the surface diffusion rate of the reactants, which in turn determines the spatial distribution of the reactants on the surface. Analytical expressions for the overall reaction rate can be derived for two limiting cases known as the "mean-field approximation" and the "nucleation and growth model". One of the assumptions of the mean-field approximation is that reactants are perfectly mixed on the surface and the reaction rate is proportional to the average coverages of the reaction partners.[9] This assumption is reasonable if the surface diffusion is much faster than the reaction itself. In the nucleation and growth model, the reacting species are considered immobile. In the case of a surface predosed with a saturated adlayer of CO, the adsorption of OH proceeds via "nucleation" at certain places, for instance at defects in the CO adlayer. The reaction takes place only at the interface between the two reacting phases, causing the formation and growth of islands. The time dependence of the nucleation determines whether the instantaneous or the progressive nucleation and growth mode operates,[25] i.e., whether the number of nucleation centers is constant or increases with time.

For diffusion rates comparable with the reaction rate, a full numerical solution of the kinetic equations is required. In this case, one either resorts to so-called Dynamic Monte Carlo simulations[16,26,27] or to a differential-equation approach involving a more advanced approximation than the mean-field model.[28]

From the experimental point of view, the most suitable technique for a quantitative study of the reaction kinetics of CO adlayer electrooxidation is chronoamperometry or potential-step experiments, which have been employed in a number of studies.[14,15,16,23,29−33] Despite the many studies devoted to CO electrooxidation there is still a lack of consensus regarding the most adequate kinetic model for describing the electrooxidation of adsorbed CO. Some authors have found that the reaction kinetics can be treated within the mean-field approximation,[31,33] while others have adhered to the nucleation and growth model to describe the experimental data.[14,29] Furthermore, little is known about the most adequate kinetic description in the presence of a low number of defects or active sites. One may expect an important role of CO surface mobility when the number of active sites for oxidation is low. Hence, very flat surfaces and highly defected surfaces may require different kinetic descriptions.

The present work reports a chronoamperometric study of the kinetics of the electrochemical oxidation of CO adlayers on a number of Pt[n(111)×(111)] surfaces. Our aim is 2-fold: first, to compare the mean-field and nucleation and growth description of the current transients, and to provide quantitative kinetic parameters of the reaction, including their potential dependence. Second, to elucidate qualitatively and quantitatively the effect of monatomic steps on the mechanism and kinetics of this model reaction. Three stepped Pt surfaces, Pt(15 15 14) with a terrace width $n = 30$, Pt(554) $n = 10$, and Pt(553) $n = 5$ were employed to span a range from relatively low to high step densities. Pt(111) and Pt (110) were included in the series as the two limiting surfaces in the [1$\bar{1}$0] zone.

2. Experimental Section

A number of bead-type single crystals of Pt[n(111)×(111)] (or equivalently Pt[(n−1)(111)×(110)]) orientation, prepared according to the Clavilier method,[34] was used in this study. Before each experiment the electrodes were flame annealed and cooled to room temperature in a H_2+Ar atmosphere. In the case of Pt(110), special care was taken to follow the procedure described in ref 35 in order to produce the unreconstructed Pt(110)-(1 × 1) surface. After flame annealing the single-crystal electrodes were transferred to the cell under the protection of a droplet of deoxygenated water and a constant potential of −0.06 V vs RHE was applied for 1 min as this pretreatment was shown to result in highly ordered stepped Pt surfaces.[36]

A platinum wire was used as a counter electrode and a saturated $Hg/Hg_2SO_4/K_2SO_4$ electrode, connected via Luggin capillary, as a reference. However, all potentials quoted were converted to the RHE scale.

The conventional glass cell and other glassware were cleaned by boiling in a mixture of concentrated nitric and sulfuric acid (1:1), followed by repeated boiling with ultrapure water.

A 0.5 M H_2SO_4 working solution was prepared from concentrated H_2SO_4 (Merck, "Suprapur") and ultrapure MilliQ water (18.2 M Ω cm, 2 ppb total organic carbon). Argon (N50) was used to deoxygenate all solutions and CO (N47) to dose CO.

Adsorption of CO was performed from a flow of ca. 15% of CO in Ar over the solution, while the working electrode was kept in the meniscus mode at 0.1 V. After the formation of a saturated adlayer of CO, as indicated by the drop of the displacement current to zero,[37] Ar was bubbled through the solution for at least 15 min to remove traces of dissolved CO, while the working electrode was kept at 0.1 V in the bulk of the solution. Then the working electrode was brought back to the meniscus mode and the oxidation of CO adlayer was initiated by stepping the potential to $E_{step} > 0.7$ V, with the current transient being recorded simultaneously. After the current had dropped to zero in the transient, a blank profile of the working electrode was recorded to check for a possible readsorption of CO or contamination. Normally, no changes in the blank profile of the electrodes after CO was oxidized off were observed, and a current transient was accepted for further data processing only if the cleanliness requirements, defined previously by the parameters R_{hkl},[12] were met.

Measurements were performed at constant temperature (25 °C) with the help of a computer-controlled Autolab PGSTAT20 potentiostat.

The CO coverages were calculated taking into account corrections for (bi)sulfate adsorption on the Pt(hkl) electrode in accordance with data obtained by the charge displacement technique.[36,38]

3. Results and Discussion

3.1. Structure of the Pt[n(111)×(111)] Surfaces and Their Voltammetric Profiles in CO-Free Electrolyte. The [n(111)×(111)] surfaces (or equivalently [(n−1)(111)×(110)]) for an fcc metal are composed of terraces of (111) orientation, which are (n−1)-atoms wide, separated by monatomic steps of (110) orientation (see Figure 1 [39]). These vicinal planes were found to be stable and have their nominal surface structure both under the UHV conditions[6c] and in air.[40] The specific spatial distribution of the electrons of the stepped surfaces is known to result in significantly lower local work function at the step sites in UHV.[41] Recently, it has been shown that these remarkably large differences in local work functions between Pt steps and terraces are not attenuated greatly by the presence of the aqueous ambient.[36] The quantitative agreement of the changes in the potential of zero change as a function of step density with the changes in work function observed in a vacuum, also attests to the equivalence of the surface structures of Pt[n(111)×(111)] in the two environments.

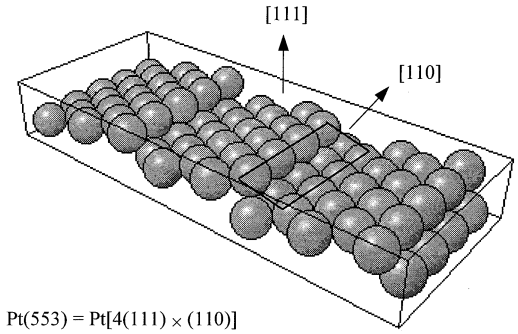

Figure 1. Schematic representation of Pt(553) to illustrate the structure of the Pt[n(111)×(111)] surfaces.[39]

It is well-known that voltammetric profiles of Pt(*hkl*) in supporting electrolyte can be considered as a fingerprint of the crystalline structure of the platinum single crystals due to the high structure sensitivity of the water reduction and oxidation and anion adsorption and desorption processes. The crystal orientation itself, i.e., the *hkl* indices, the amount and type of crystalline defects, and also the degree of cleanliness of the system can be derived from the blank cyclic voltammogram.

Cyclic voltammograms of the stepped surfaces Pt(553), Pt(554), and Pt(15 15 14) with 5-, 10-, and 30-atoms wide terraces, respectively, Pt(111) and Pt(110) are shown in Figure 2. The profiles are in good agreement with previously published data[36,42−45] confirming the surface crystalline order of the electrodes and the cleanliness of the system.

A characteristic voltammetric feature of the Pt single crystals of [n(111)×(111)] orientation (or, equivalently, [(n−1)(111)×(110)]) is a sharp peak at 0.125 V. The charge under this peak is proportional to the step fraction $\theta_{step} = 1/n$, and corresponds to the transfer of ca. 1 electron per step edge atom as was reported previously.[42,43] Figure 3 shows this dependence for the electrodes used in the present study. The peak was therefore concluded to originate from hydrogen adsorption on (110) steps and can be used as a direct measure of the number of such step sites.[42,43]

Note that as a measure of the number of active sites we use the step fraction 1/n, quantity which is related to the number of surface atoms, rather than step density $2/\sqrt{3}d(n - {}^2/_3)$,[42,43] which is related to the surface area.

It can be seen in Figure 2a that our Pt(111) crystal also has a small amount of (110) defects as evidenced by a hump at 0.125 V. The charge density under this peak is 1.2 μC/cm^2, which corresponds to θ_{step} of 0.0034 ML as extrapolated from the linear fit of Figure 3. This would correspond to the terraces of approximately 300 atoms wide, proving the high quality of our Pt(111) crystal.

There is apparently a small amount of sites of (100) orientation on the surface of our Pt(15 15 14) crystal as can be judged from the appearance of the peak at ca. 0.27 V (Figure 2a). The (100) defects could originate from a small distortion of the (110) steps, as it has been reported in other cases of stepped surfaces.[46] However, the charge under this peak constitutes only 14% of that for (110) steps and hence is not expected to be of significant importance. In the following, Pt(15 15 14), Pt(554), and Pt(553) are assumed to have their nominal θ_{step} of 0.033, 0.1, and 0.2 ML, respectively.

Determination of the θ_{step} for Pt(110) is not that straightforward since this basal plane is known to reconstruct to adopt either the Pt(110)-(1×1) structure (with formally $\theta_{step} = 0.5$) or the Pt(110)-(1×2) "missing row" configuration (with formally $\theta_{step} = 0.33$ ML). It has been shown using in situ X-ray scattering that under certain conditions of the flame annealing and cooling of the Pt(110) electrode the unreconstructed (1×1) surface is formed.[35,47] No reconstruction of Pt(110)-(1×1) upon immersion into the electrolyte was observed and this surface was shown to be stable in the potential region from 0 to 1 V.[35,47] Unlike Pt(110) in UHV, adsorption and oxidation of CO was also not found to cause reconstruction of the Pt(110)-(1×1) surface.[35,47] The blank profile of the Pt(110) electrode, prepared following the procedure described by Marković et al.,[35] is shown in Figure 2c. The observation of negligible current densities at potentials higher than 0.2 V and the sharpness of the main peak, with a peak current higher than 400 μA cm^{-2}, suggest that this electrode pretreatment lead to an optimal voltammetric profile.[44] The profile agrees well with those reported by other groups, who employed the same protocol for Pt(110) preparation[44,45] and allows us to conclude that our preparation procedure resulted in the Pt(110)-(1×1) surface.

3.2. CO Oxidation. The chronoamperometric measurements of the oxidation of a saturated adlayer of CO were performed for all Pt single crystals at a number of final potentials. The corresponding current transients are shown in Figure 4. All the transients have a similar shape: after charging of the double layer (a high current at short times) there is a current plateau followed by a main peak.

The charge under the transient for a given surface is found to be independent of the final potential and corresponded to a CO coverage of 0.64 ± 0.02 ML for Pt(111), 0.66 ± 0.1 ML for Pt(15 15 14), 0.63 ± 0.05 ML for Pt(554), 0.66 ± 0.02 ML for Pt(553), and 0.90 ± 0.03 ML for Pt(110). Our results agree well with the previously reported saturation coverages of CO on Pt[n(111)×(111)], obtained under similar experimental conditions.[48]

From the analysis of the current transient it is clear that in the region of the main peak the reaction is a second-order process with respect to CO coverage.[31,33] However, the apparent reaction order in the current plateau region with respect to adsorbed CO is either zero or "quasi zero".[33] This suggests that the reaction mechanism in the plateau region is different from that in the main peak. Therefore, we will discuss this process first before discussing the main oxidation peak.

3.2.1. Current Plateau Region. The current in the plateau region is found to depend on step density (Figure 5). The major enhancement of the rate of the CO adlayer oxidation in the plateau region is observed when passing from Pt(111) to Pt(15 15 14), the plateau current increasing by 1 order of magnitude. Further increase of the step density does not lead to a significant rise of the current in the plateau region. In fact, the rate of the reaction initiation on Pt(554) is the same as that on Pt(15 15 14) and is only slightly lower than on Pt(553) and Pt(110) (see Figure 5). This points out the extraordinary role of a small amount of defect sites in the oxidation initiation step.

For all Pt electrodes the current in the plateau region is found to increase with increasing final potential, the plot of the logarithm of the current versus the final potential being linear with a slope of 81 ± 4 mV/dec for Pt(111), 82 ± 3 mV/dec for Pt(15 15 14) and Pt(554), and 111 ± 15 mV/dec for Pt(553) and Pt(110) (Figure 5). A change in the Tafel slope with increasing step density could reflect a change in the rate determining step from the chemical step 2 on electrodes with large (111) terraces to the first electron transfer 1 on electrodes with high density of (110) step sites.

Similarly to the present work, a current plateau prior to the main peak of the transient was observed in a number of previous studies on the kinetics of the CO adlayer oxidation.[14,31−33] It

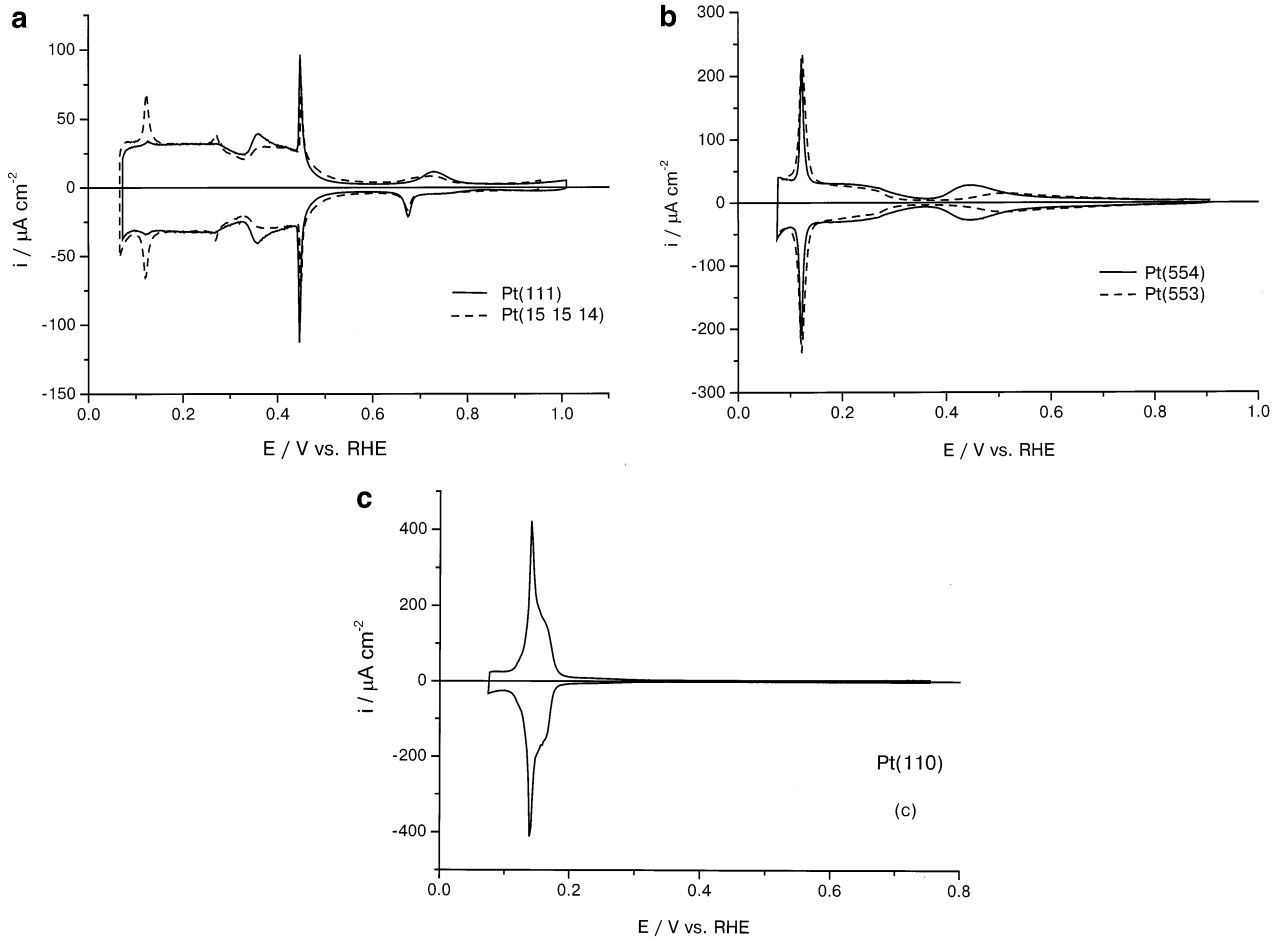

Figure 2. Cyclic voltammograms of different Pt surfaces in 0.5M H_2SO_4, sweep rate 50 mV/s, $T = 25$ °C. (a) Pt(111) and Pt(15 15 14), (b) Pt(554) and Pt(553), and (c) Pt(110).

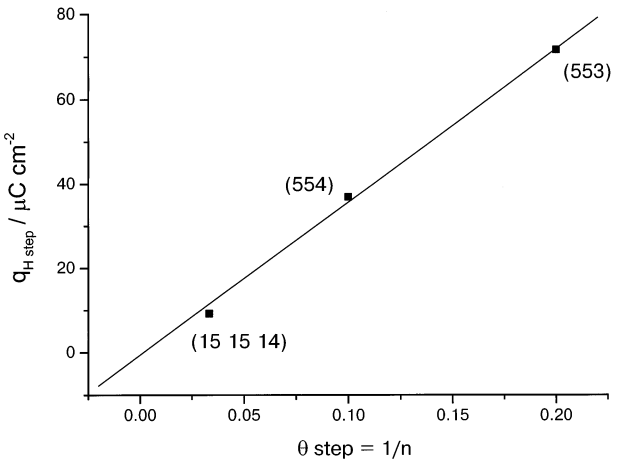

Figure 3. Charge density of the hydrogen adsorption on (110) steps in 0.5M H_2SO_4 plotted versus the step fraction. Solid line is a least-squares fit of the data, demonstrating a linear dependence.

has been suggested by Bergelin et al.[31] that the constant current results from the incipient oxidation of the saturated CO adlayer by an Eley−Rideal mechanism, which involves a reaction of adsorbed CO with a neighboring nonadsorbed water molecule. However, Akemann et al. observed that the current in the plateau region depends on the Pt(111) crystal preparation and varies markedly for different Pt(111) crystals.[32] Therefore, this process was assigned to the oxidation of CO adsorbed in the vicinity of defects and steps.[32]

As we discussed in our previous paper,[33] the dependence of the plateau current on the defect density makes an Eley−Rideal type of reaction initiation rather unlikely and points toward a Langmuir−Hinshelwood mechanism. Since the current in the plateau region does not increase linearly with the step density (Figure 5), a Langmuir−Hinshelwood mechanism involving noncompetitive adsorption of OH on defects and CO on adjacent sites does not seem consistent with the experimental data. However, other effects as, for example, a change in the rate determining step of the mechanism with increasing step density, may mask and complicate the expected dependence. Another possible mechanism of the reaction in the current plateau region was proposed in our previous paper:[33] it involves a Langmuir−Hinshelwood mechanism with no effective freeing of sites for OH adsorption as the first few CO molecules are oxidized, due to the relaxation of the CO adlayer upon removal of these first CO molecules. The critical role of crystalline defects in the reaction initiation indicates that, indeed, the reaction is initiated at the steps (Figure 5), most probably due to a preferential adsorption of OH at those sites. As we discussed in our previous paper,[33] the pronounced dependence of the reaction initiation rate on the density of the crystalline defects in the limit of low θ_{step}, i.e., for Pt(111), may well account for the discrepancy in the results of different groups since the quality of the crystals may vary. Crystal quality is of utmost importance as the kinetics of both reaction initiation and the main oxidation peak depend sensitively on the defect density. However, we would like to point out that at present still little is known about the

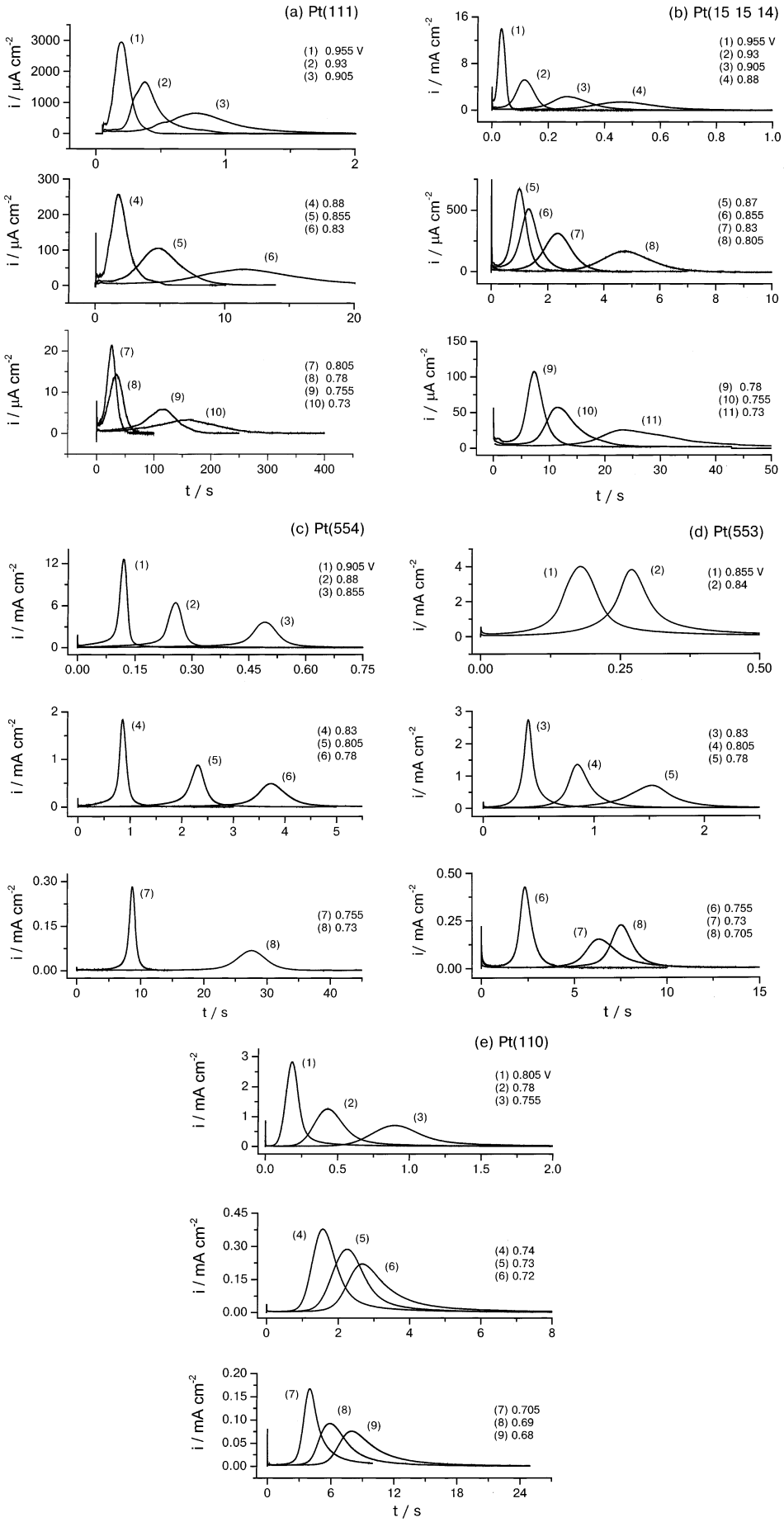

Figure 4. Current transients of the oxidation of saturated CO adlayers on (a) Pt(111), (b) Pt(15 15 14), (c) Pt(554), (d) Pt(553), and (e) Pt(110). Final potential is indicated in the figure.

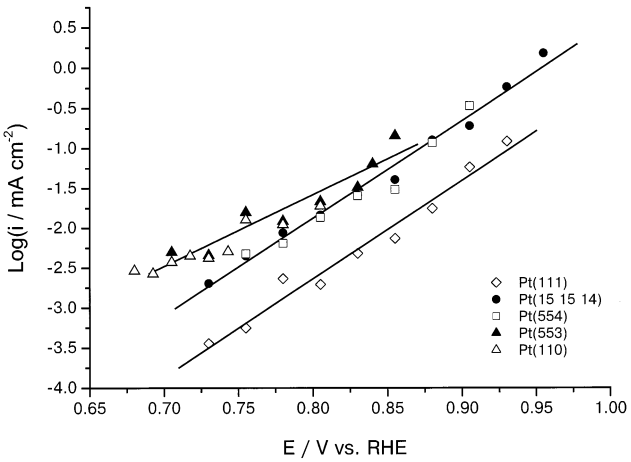

Figure 5. Logarithm of the current in the plateau region versus the final potential for Pt(111), Pt(15 15 14), Pt(554), Pt(553), and Pt(110). Solid lines are the least-squares fits of the data.

initiation of the CO oxidation reaction and this issue deserves further investigation.

3.2.2. The Main Peak of the CO Oxidation. Once the reaction is initiated, the oxidation of CO proceeds via a Langmuir−Hinshelwood mechanism as can be concluded from the peaked shape of the current transients (Figure 4). The promoting effect of steps on the CO oxidation rate is obvious: the higher the step density the faster the reaction. For example, it takes approximately 300 s to complete oxidation of a saturated CO adlayer on Pt(111) at 0.73 V, while on Pt(110) only ca. 5 s are required even though the saturation coverage of CO on Pt(110) is higher (Figure 4). Our results are in line with previous observations of enhanced activity toward CO oxidation of surfaces with an increased defect density.[12,14−16,18,33]

The shape of the transients changes slightly with the density of steps. For the surfaces with low step density, Pt(111), Pt(15 15 14), and Pt(554), the main peak is symmetric, while for Pt(553) and especially Pt(110), a tailing on the descending part of the transient is observed (see Figures 4 and 6). The likely origin of the tailing is discussed below.

Despite this variation of the transient shape, the main peak can be fitted satisfactorily by a mean field model in the entire range of step potentials and for all Pt[n(111)×(111)] surfaces (examples are shown in Figure 6), using the expression[31]

$$i(t) = \frac{Qk \exp(-k(t - t_{max}))}{[1 + \exp(-k(t - t_{max}))]^2} \qquad (4)$$

where $i(t)$ is the current density, Q is the charge associated with the oxidation of the CO adlayer in the main peak region (including readsorption of (bi)sulfate), k is the reaction rate constant for reaction 2 (the only fitting parameter in the model), and t_{max} is the time at which the maximum current is observed in the transient. This expression is derived from reactions 1−3 assuming that the formation of the oxygen-containing species is reversible, so that its coverage θ_{OH} is always proportional to $(1 - \theta_{CO})$. This assumption seems reasonable since the incipient oxidation of the Pt surface is known to be reversible.[49]

The nucleation and growth model gives a fit of the transients which is significantly inferior to that of the mean-field model. Instantaneous nucleation and growth can be ruled out since the ascending part of the transients is clearly not linear, and progressive nucleation and growth results in noticeably broader transients (dashed lines in Figure 6). Note that the differences between both models in the main peak region are more clearly reflected on stepped surfaces than on the well ordered Pt(111). Thus, it appears that the validity of the mean-field Langmuir−Hinshelwood model is better demonstrated on surfaces having a controlled amount of surface defects. As was pointed out above, a slight tailing on the descending part of the transients for electrodes with high step density (Pt(553) and Pt(110)) was observed. Neither the mean-field model nor the nucleation and growth model are able to reproduce this part of the transient exactly.

To investigate whether the tailing of the current transients for surfaces with a high step density could be related to a slow diffusion of CO on the terraces, we simulated the reaction kinetics by solving the kinetic differential equations numerically. Our model includes the following assumptions. The stepped surface consists of terraces of width L. On the terraces CO is adsorbed, which can diffuse along the terrace following macroscopic diffusion laws (see insert in Figure 7). The change in the CO coverage with time is then given by the Fick's second law:

$$\frac{\partial\theta}{\partial t} = D\frac{\partial^2\theta}{\partial x^2}$$

where θ is CO coverage, t is time, and D the diffusion coefficient and x the spatial coordinate. The CO oxidation reaction can only take place at one side of the step, for example, at coordinate $x = 0$, such that one of the boundary conditions is

$$D\frac{\partial\theta}{\partial x} = -k\theta(1 - \theta) \qquad \text{at} \qquad x = 0$$

where k is the rate constant of the Langmuir−Hinshelwood surface reaction. (Note that this second-order rate law means that at $x = 0$ the adsorption of CO and OH is competitive.)

Since there is diffusion of CO only along the terrace and there is no mass-transfer across the step (see for example, ref 3), the boundary condition at the other terrace side $x = L$ is set at

$$D\frac{\partial\theta}{\partial x} = 0 \qquad \text{at} \qquad x = L$$

Finally, the initial condition is

$$\theta = \theta_0 \qquad \text{at} \qquad t = 0 \text{ and all coordinates.}$$

Introducing the new dimensionless variables $\bar{x} = x/L$ and $\bar{t} = tD/L^2$ and the parameter $K = kL/D$, the initial system of differential equations can be simplified to a system with only one parameter, namely, K

$$\frac{\partial\theta}{\partial\bar{t}} = \frac{\partial^2\theta}{\partial\bar{x}^2}$$

$$\frac{\partial\theta}{\partial\bar{x}} = -K\theta(1 - \theta) \qquad \text{at} \qquad \bar{x} = 0$$

$$\frac{1}{K}\frac{\partial\theta}{\partial\bar{x}} = 0 \qquad \text{at} \qquad \bar{x} = 1$$

$$\theta = \theta_0 \qquad \text{at} \qquad \bar{t} = 0 \text{ and for all } \bar{x}$$

This set of equations can be solved numerically for different values of K. Some calculated current transients are shown in Figure 7. A tailing in the transient is observed, which becomes more pronounced with increasing K, i.e., increasing terrace width

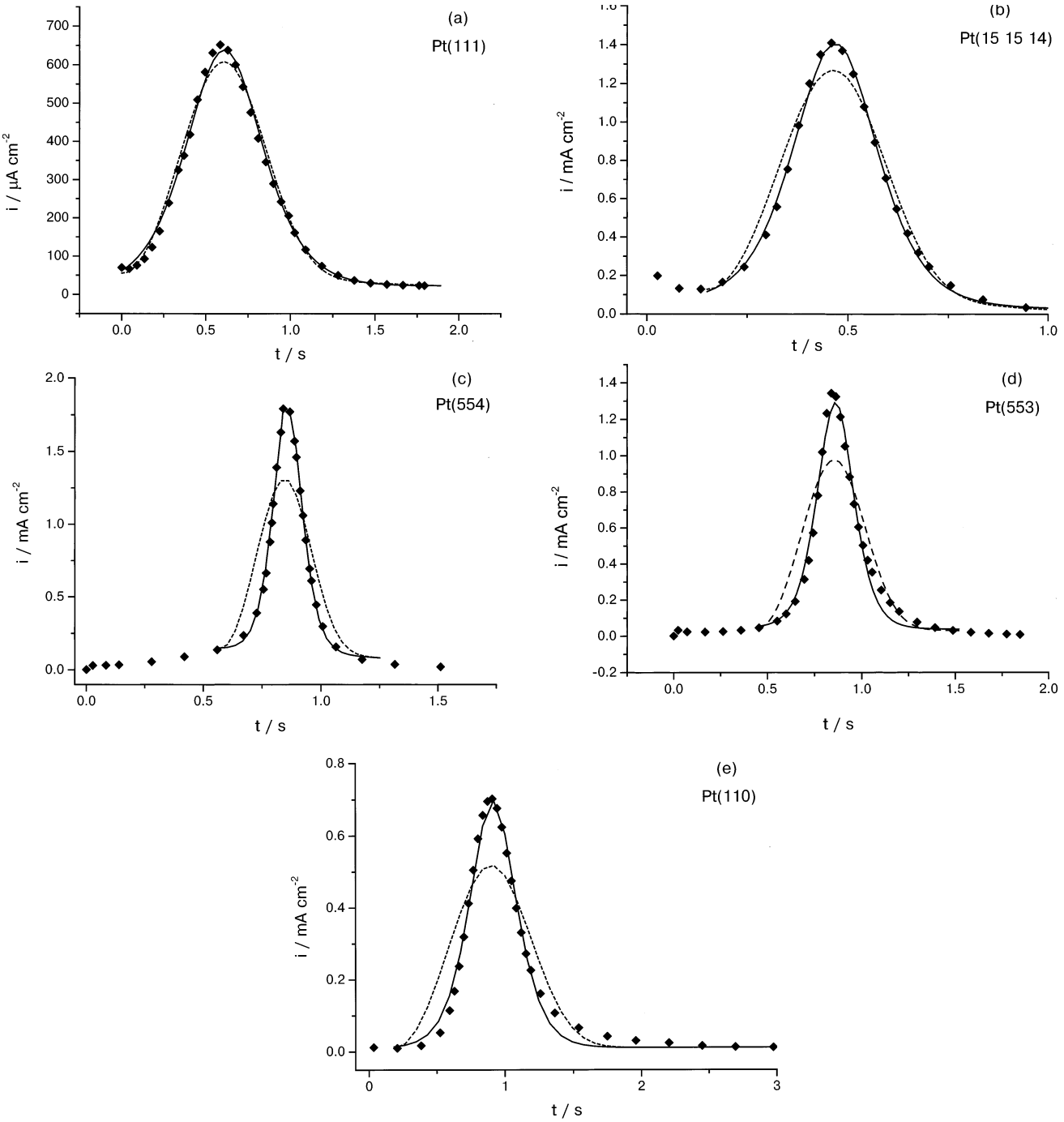

Figure 6. Current transients for CO adlayer oxidation on (a) Pt(111) at final potential $E_f = 0.905$ V, (b) Pt(15 15 14) at $E_f = 0.88$ V, (c) Pt(554) $E_f = 0.83$ V, (d) Pt(553) $E_f = 0.805$ V, and (e) Pt(110) $E_f = 0.755$ V. Experimental data (diamonds), fit by mean-field approximation (eq 6) (solid line), fit by the progressive nucleation and growth model (dashed line). Only a few experimental data points are depicted for the sake of clarity.

L, faster reaction *k*, or slower diffusion *D*. Assuming the diffusion coefficient of CO on the (111) terrace to be independent of the step density, as it was observed experimentally for Pt stepped surfaces under UHV conditions,[50−54] we can conclude that in case of slow diffusion of CO the tailing in the transient should be easier to observe for surfaces with large terraces. By contrast, experimentally we observe an increased tailing for surfaces with relatively narrow terraces, which indicates that the tailing does not originate from a slow diffusion of CO but from a different phenomenon.

Recent in situ FTIR measurements of the CO adlayer oxidation on stepped Pt surfaces have suggested that CO adsorbed on terraces reacts faster than that on steps.[55] Therefore, the tailing is likely to be related to the slow oxidation of the CO molecules that remain on the steps after the oxidative removal of CO from terraces.[55,56] Since the fraction of CO molecules on steps is less than 20% even for Pt(553), we believe that the observed tailing does not undermine the mean-field model. Therefore, the apparent rate constants k_{hkl} for reaction 2 for all Pt[n(111)×(111)] electrodes and all final potentials were determined by fitting the experimental transients *i(t)* with eq 4. The determined apparent reaction constants lie in the range from $10^{-2}-10^{2}$ s^{-1} depending on the potential and step density.

Since the kinetics of the reaction in the region of the peak is well described by a mean-field approximation under our experimental conditions (Figure 6), we conclude that CO must be very mobile on the (111) terraces of all Pt[n(111)×(111)] surfaces. For Pt(110) it would be more appropriate to assume

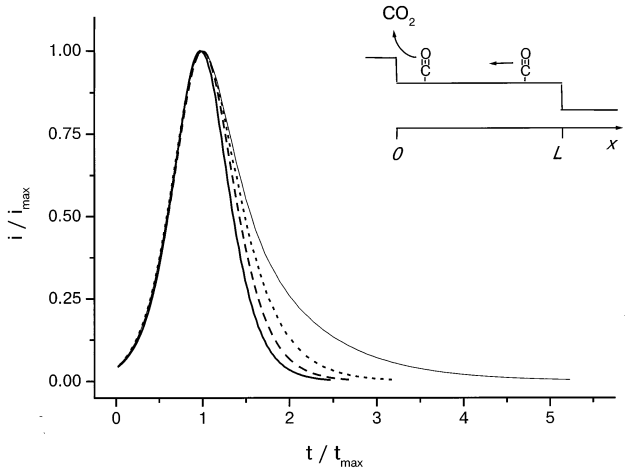

Figure 7. Numerically calculated current transients to simulating the effect of slow diffusion of CO along the terrace. $K = 0.1$ (solid thick line), $K = 1$ (dashed line), $K = 3$ (dotted line), and $K = 10$ (solid thin line). Inset shows schematically the model as discussed in detail in the text.

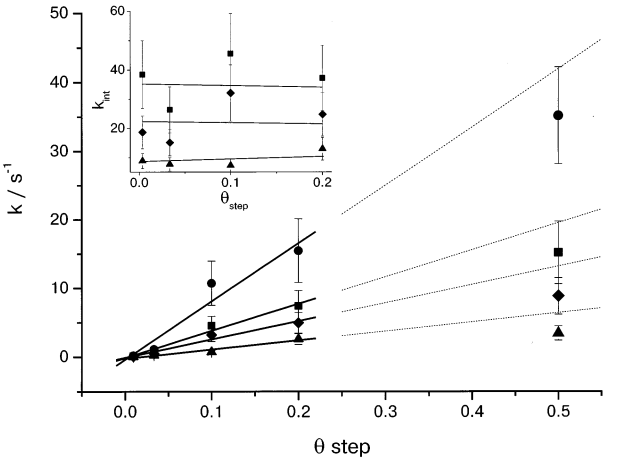

Figure 8. Dependence of the apparent rate constants, determined by fitting the experimental data with eq 6, on the step fraction. Final potentials are: 0.73 V (triangles), 0.755 V (diamonds), 0.78 V (squares), and 0.805 V (circles). The value of θ_{step} for Pt(111) was estimated using the procedure described in the section 3.1.1. Indicated experimental errors are standard deviations, determined from at least 3 measurements. Insert shows the independence of the apparent "intrinsic" rate constant of the step fraction.

fast diffusion along the [$\bar{1}$10] direction. The mobility of CO under electrochemical conditions and hence the appropriate kinetic model for CO oxidation was a central issue of many previous experimental [14,15,29,31−33] as well as theoretical [26,27] studies. From comparing current transients to either mean-field or nucleation and growth models most authors concluded that CO mobility under the electrochemical conditions is low,[14] while Bergelin et al.[31] and our previous paper[33] suggested a high diffusion rate of CO on the Pt(111) electrode surface. A low mobility of CO on the electrode surface, and hence nucleation and growth kinetics of the CO adlayer oxidation, would be consistent with the formation of CO islands during the oxidation as inferred from in situ IR spectroscopy.[57] On the other hand, under UHV conditions diffusion of CO on platinum (111) terraces is known to be very fast,[50−53] with a typical hopping rate on the order of 10^5 s^{-1} at 195 K and low CO coverage [50−52] and 10^7 s^{-1} at 300 K and CO coverage of 0.67 M.[53] From reviewing over 500 systems Seebauer et al. concluded an apparent insensitivity of diffusional parameters to the presence of an aqueous ambient,[54] which suggests that a high hopping rate of CO should be expected under electrochemical conditions as well. Having determined the apparent rate constant k of CO oxidation and taking into account that $K = k(L/D)$ should be lower than 0.1 for the mean-field approximation to be valid (vide supra), the apparent diffusion coefficient of CO on (111) terraces can be estimated. Since the diffusion is fast enough even at highest reaction rate on Pt(15 15 14), the surface with the largest terraces of approximately 70 Å width, the following expression is applicable: $K = 10^2\ s^{-1}(7 \times 10^{-7}\ cm\ /D) < 0.1$, from which the one-dimensional diffusion coefficient $D > 7 \times 10^{-4}$ cm/s. The corresponding two-dimensional diffusion coefficient, $D_2 = a_0 D/4$, where a_0 is a lattice constant,[52] is then $D_2 > 10^{-11}$ cm^2/s. This, in turn, would correspond to the hopping rate of 10^5 s^{-1}, which is, taking into account the very approximate character of the present estimation, in good agreement with the hopping rate of CO on (111) terraces in UHV. From their kinetic measurements of the CO oxidation on a Ru modified Pt(111) electrode, Friedrich et al. estimated the lower limit value for the CO diffusion coefficient to be ca. 4×10^{-14} cm^2/s.[58] However, from the comparison with the corresponding measurements of Gasteiger et al.[59] they concluded that the mobility of CO is significantly higher than the calculated lower limit, namely in the range of 10^{-13}−10^{-12} cm^2/s.[58] This is further supported by the present study.

Although our macroscopic kinetic study of the electrochemical oxidation of a CO adlayer indicates that the reaction follows a Langmuir−Hinshelwood mechanism under the mean-field approximation, the issue of the active site for this reaction remains. Given the results of the present study, the role of the crystalline defects in catalyzing the CO oxidation can be analyzed quantitatively. Figure 8 shows the dependence of the apparent rate constant on the fraction of the step atoms for a number of final potentials. It can be seen that for the surfaces with θ_{step} lower than 0.2, i.e., for Pt(111), Pt(15 15 14), Pt(554), and Pt(553), the apparent rate constant increases linearly with θ_{step}. However, the apparent rate constant for the CO oxidation on Pt(110) is always slightly lower than the one extrapolated from a linear fit at $\theta_{step} < 0.2$. We believe this deviation could originate from the higher binding energy of CO on Pt(110) compared to Pt(111) at all CO coverages,[60,61] which may increase the activation barrier for oxidation and hence lower the rate constant. On the other hand, there is the question of the correct definition and determination of the step fraction for Pt(110), although this surface is believed to be unreconstructed and hence formally have $\theta_{step} = 0.5$ ML. For surfaces with relatively low step density ($\theta_{step} < 0.2$) the following expression for the apparent rate constant can be suggested:

$$k^{hkl}_{apparent}(E_{final},\theta_{step}) = k_{intrinsic}(E_{final}) \times \theta_{step} \qquad (5)$$

where $k^{hkl}_{apparent}(E_{final},\theta_{step})$ is the apparent rate constant of the reaction 2, determined via fitting an experimental transient for Pt(hkl) with the mean-field model and $k_{intrinsic}$ (E_{final}) is the apparent "intrinsic" rate constant of the same reaction, i.e., the rate constant for the reaction taking place on the (110) step. The apparent "intrinsic" rate constant for the CO oxidation on (110) step, determined from the eq 5, lies in the range from 10 to 10^3 s^{-1} depending on the potential.

Several important conclusions can be drawn from this finding:

(1) Steps are indeed the active sites for the CO oxidation on Pt[n(111)×(111)]. The reaction preferably takes place at the steps (at least in the potential region studied), while the terraces seem to merely supply CO through fast surface diffusion.

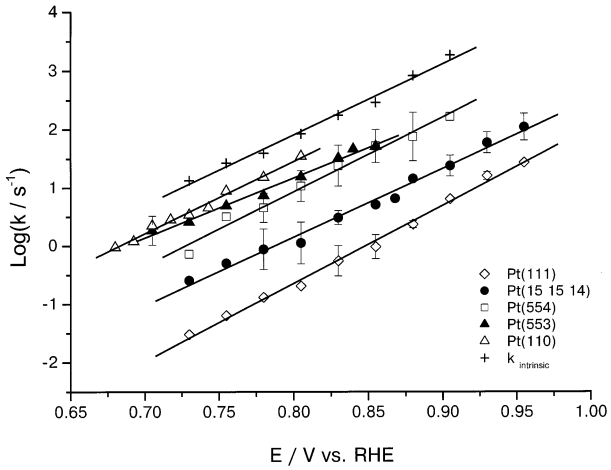

Figure 9. Dependence of the apparent rate constants, determined by fitting the experimental data with eq 6, and the apparent intrinsic rate constant on the potential. Pt(111), Pt(15 15 14), Pt(554), Pt(553), Pt(110), and apparent intrinsic rate constant. Only the highest relative experimental errors are indicated.

Importantly, the reaction would not occur on an ideal atomically flat Pt(111) surface in the potential region studied. We believe that the reason for the enhanced reactivity of steps is the preferential adsorption of oxygen-containing species at the steps for a surface predosed with CO.[12]

We realize, however, that macroscopic kinetic measurements do not provide detailed information on the nature of the electrocatalyst active site, i.e., the number of surface atoms involved in the elementary reaction, their geometric arrangement etc. Our complementary in situ FTIR study will show that the sites at the bottom of the step and not the step edges are active in the CO oxidation.[55]

(2) The intrinsic catalytic activity of the steps $k_{\text{intrinsic}}$ does not depend on the step density for surfaces with $\theta_{\text{step}} < 0.2$ (see insert in Figure 8). This essentially means that for $\theta_{\text{step}} < 0.2$ the effect of steps on the reaction rate is additive.

The dependence of the apparent rate constant $k^{hkl}_{\text{apparent}}$ and the apparent intrinsic rate constant $k_{\text{intrinsic}}$ on the potential is exponential, as shown in Figure 9. The potential dependence of the apparent rate constants, determined from the Figure 9, is essentially independent of the step density: 75 ± 3 mV/dec for Pt(111), 85 ± 3 mV/dec for Pt(15 15 14), 78 ± 4 mV/dec for Pt(554), 97 ± 4 mV/dec for Pt(553), and 81 ± 3 mV/dec for Pt(110). The potential dependence of the apparent intrinsic rate constant is also close to these values, namely, 83 ± 3 mV/dec. Assuming that the exponential dependence of the apparent rate constant on potential holds at lower overpotentials and the mechanism of the reaction does not change, the extrapolated $k_{\text{intrinsic}}$ at 0 V is ca. 10^{-8} s^{-1}, which clearly demonstrates a very slow reaction at potentials close to the standard potential for CO oxidation. The indifference of the Tafel slope to the surface structure could suggest that CO oxidation follows the same mechanism on all surfaces studied. A very similar Tafel slope for the apparent rate constant of 72 mV/dec was found by Bergelin et al.[31] for the CO oxidation on Pt(111), using an impinging jet technique. Although Lipkowski et al. concluded a nucleation and growth mechanism for the electrochemical CO oxidation, the growth rate constant (essentially CO oxidation rate constant) at low final potentials was shown to be surface−structure independent and have a similar Tafel slope of about 80 mV/dec[14] Tafel slopes of about 60−80 mV/dec were also found in potentiodynamic studies of the oxidation of CO adlayers.[62,63] The value of the Tafel slope being relatively close to 60 mV/dec can be interpreted in terms of a slow chemical step 2 in the reaction mechanism (reactions 1−3). Recent detection of a $COOH_{ads}$ species in the electrochemical oxidation of a CO adlayer on Pt using FTIRS with attenuated total reflection would support this conclusion.[64] Nevertheless, further research is required in order to establish the mechanism unambiguously.

4. Conclusions

The kinetics of the electrochemical oxidation of a CO adlayer on Pt[n(111)×(111)] electrodes, with $n = 30$, 10, and 5, and Pt(111) and Pt(110) electrodes in 0.5 M H_2SO_4 has been studied using chronoamperometry, with the objective of elucidating quantitatively the effect of steps on the reaction kinetics and mechanism.

In the oxidation of a saturated CO adlayer two processes can be distinguished in the current transients: a reaction initiation that appears to be an apparently zeroth-order process, followed by the main oxidation process, which is shown to be of the Langmuir−Hinshelwood type with a competitive adsorption of the two reactants, CO and OH.

The reaction kinetics in the main peak region can be modeled well using the mean-field approximation for the Langmuir−Hinshelwood mechanism (reactions 1−3), which implies fast diffusion of CO adsorbed on the terraces of Pt[n(111)×(111)] surfaces under electrochemical conditions. The surface diffusion coefficient of CO is estimated to be higher than 10^{-11} cm^2/s.

The apparent rate constants for the electrochemical CO oxidation on Pt[n(111)×(111)] were determined by fitting the experimental data with the mean-field model. The determined apparent reaction constants lie in the range from 10^{-2} to 10^2 s^{-1} depending on the potential and step density.

At a given potential the apparent rate constant k is shown to be proportional to the step fraction for the Pt[n(111)×(111)] surfaces with n > 5, giving quantitative proof of the assertion that steps are the active sites in the CO oxidation on platinum. The reaction preferably takes place at the steps (at least in the potential region studied), while the terraces merely supply CO through fast surface diffusion. Significantly, the reaction would not take place on an ideal atomically flat Pt(111) surface in the potential region studied. The role of steps is thus to preferentially adsorb the oxygen-containing species with which CO reacts.

The intrinsic catalytic activity of the steps on the Pt[n(111)×(111)] surfaces with $n > 5$ is shown to be independent of the step density. A decrease of the apparent step reactivity for Pt(110) is presumably related to a higher binding energy of CO on this surface.[60]

The apparent intrinsic rate constant (k/θ_{step}) for the oxidation of CO on platinum was determined to be $10-10^3$ s^{-1} in the potential region studied. At the potential close to the standard potential of CO oxidation (ca. 0 V), the apparent intrinsic rate constant is extrapolated to be 10^{-8} s^{-1}, confirming the extreme sluggishness of this reaction.

The potential dependence of the apparent rate constant is found to be structure insensitive and have a Tafel slope of ca. 80 mV/dec, which is consistent with the presence of a slow chemical step 2 in an ECE reaction scheme (reactions 1−3).

Acknowledgment. This research was supported by the Royal Netherlands Academy of Arts and Sciences (KNAW), by a Spinoza grant from The Netherlands Foundation for Scientific Research (NWO), and by the Ministerio de Ciencia y Tecnologia (Spain) Grant BQU 2000-0240.

References and Notes

(1) Somorjai, G. A. *Introduction to Surface Chemistry and Catalysis*; John Wiley & Sons: New York, 1994.

(2) Boudart, M. *Adv. Catal.* **1969**, *20*, 153.

(3) Yates, J. T., Jr. *J. Vac. Sci. Technol. A* **1995**, *13*, 1359.

(4) Hammer, B.; Nørskov, J. K. *Adv. Catal.* **2000**, *45*, 71.

(5) Tersoff, J.; Falicov, L. M. *Phys. Rev. B* **1981**, *24*, 754.

(6) (a) Hayden, B. E.; Kretzschmar, K.; Bradshaw, A. M.; Greenler, R. G. *Surf. Sci.* **1985**, *149*, 394. (b) Luo, J. S.; Tobin, R. G.; Lambert, D. K.; Fisher, G. B.; DiMaggio, C. L. *Surf. Sci.* **1992**, *274*, 53. (c) Hahn, E.; Fricke, A.; Roder, H.; Kern, K. *Surf. Sci.* **1993**, *297*, 19. (d) Hammer, B.; Nielsen, O. H.; Nørskov, J. K. *Cat. Lett.* **1997**, *46*, 31.

(7) (a) Gland, J. L.; Korchak, V. N. *Surf. Sci.* **1978**, *75*, 733. (b) Feibelman, P. J.; Esch, S.; Michely, T. *Phys. Rev. Lett.* **1996**, *77*, 2257. (c) Wang, H.; Tobin, R. G.; Lambert, D. K.; DiMaggio, C. L.; Fisher G. B. *Surf. Sci.* **1997**, *372*, 267.

(8) (a) Ramsier, R. D.; Gao, Q.; Neergaard Waltenburg, H.; Yates, J. T.Jr. *J. Chem. Phys.* **1994**, *100*, 6837. (b) Zambelli, T.; Wintterlin, J.; Trost, J.; Ertl, G. *Science*, **1996**, *273*, 1688. (c) Hammer, B *Faraday Discuss.* **1998**, *110*, 323. (d) Dahl, S.; Logadottir, A.; Egeberg, R. C.; Larsen, J. H.; Chorkendorff, I.; Törnqvist, E.; Nørskov, J. K. *Phys. Rev. Lett.* **1999**, *83*, 1814. (e) Hammer, B. *Surf. Sci.* **2000**, *459*, 323.

(9) Masel, R. I. *Principles of Adsorption and Reaction on Solid Surfaces*; John Wiley & Sons: New York, 1996.

(10) Gambardella, P.; Šljivančanin, Ž.; Hammer, B.; Blanc, M.; Kuhnke, K.; Kern, K. *Phys. Rev. Lett.* **2001**, *87*, 56103.

(11) (a) Kim, C. S.; Tornquist, W. J.; Korzeniewski, C. *J. Phys. Chem.* **1993**, *97*, 6484. (b) Kim, C. S.; Korzeniewski, C.; Tornquist, W. J. *J. Chem. Phys.* **1994**, *100*, 628. (c) Wang, H.; Tobin, R. G.; Lambert, D. K. *J. Chem. Phys.* **1994**, *101*, 4277. (d) Kim, C. S.; Korzeniewski, C. *Anal. Chem.* **1997**, *69*, 2349.

(12) Lebedeva, N. P.; Koper, M. T. M.; Herrero, E.; Feliu, J. M.; van Santen, R. A. *J. Electroanal. Chem.* **2000**, *487*, 37.

(13) (a) Motoo, S.; Furuya, N. *J. Electroanal. Chem.* **1984**, *172*, 339. (b) Clavilier, J.; El Achi, K.; Petit, M.; Rodes, A.; Zamakhchari, M. A. *J. Electroanal. Chem.* **1990**, *295*, 333.

(14) Love, B.; Lipkowski, J. *ACS Symp. Ser.* **1988**, *378*, 484.

(15) Santos, E.; Leiva, E. P. M.; Vielstich, W. *Electrochim. Acta* **1991**, *36*, 555.

(16) Petukhov, A. V.; Akemann, W.; Friedrich, K. A.; Stimming, U. *Surf. Sci.* **1998**, *402*−*404*, 182.

(17) Lebedeva, N. P.; Koper, M. T. M.; Feliu, J. M.; van Santen, R. A. *Electrochem. Comm.* **2000**, *2*, 487.

(18) Gómez, R.; Orts, J. M.; Feliu, J. M.; Clavilier, J.; Klein, L.H. *J. Electroanal. Chem.* **1997**, *432*, 1.

(19) (a) Motoo, S.; Furuya, N. *Ber. Bunsen-Ges. Phys. Chem.* **1987**, *91*, 457. (b) Smith, S. P. E., Ben-Dor, K. F.; Abruña, H. D. *Langmuir* **1999**, *15*, 7325.

(20) Sun, S.-G.; Chen, A.-C.; Huang, T.-S.; Li, J.-B.; Tian, Z.-W. *J. Electroanal. Chem.* **1992**, *340*, 213.

(21) Tarnowski, D. J.; Korzeniewski, C. *J. Phys. Chem. B* **1997**, *101*, 253.

(22) Beden, B.; Lamy, C.; de Tacconi, N. R.; Arvia, A. J. *Electrochim. Acta* **1990**, *35*, 691.

(23) Gilman, S. *J. Phys. Chem.* **1964**, *68*, 70.

(24) Herrero, E.; Feliu, J. M.; Blais, S.; Radovic-Hrapovic, Z.; Jerkiewicz, G. *Langmuir* **2000**, *11*, 4779.

(25) Schmickler, W. *Interfacial Electrochemistry*; Oxford University Press: New York, 1996; Chapter 10.

(26) Koper, M. T. M.; Jansen, A. P. J.; van Santen, R. A.; Lukkien, J. J.; Hilbers, P. A. J. *J. Chem. Phys.* **1998**, *109*, 6051.

(27) Petukhov, A. V. *Chem. Phys. Lett.* **1997**, *277*, 539.

(28) Koper, M. T. M.; Jansen, A. P. J.; Lukkien, J. J. *Electrochim. Acta* **1999**, *45*, 645.

(29) McCallum, C.; Pletcher, D. *J. Electroanal. Chem.* **1976**, *70*, 277.

(30) Santos, E.; Leiva, E. P. M.; Vielstich, W.; Linke, U. *J. Electroanal. Chem.* **1987**, *227*, 199.

(31) Bergelin, M.; Herrero, E.; Feliu, J. M.; Wasberg, M. *J. Electroanal. Chem.* **1999**, *467*, 74.

(32) Akemann, W.; Friedrich, K. A.; Stimming, U. *J. Chem. Phys.* **2000**, *113*, 6864.

(33) Lebedeva, N. P.; Koper, M. T. M.; Feliu, J. M.; van Santen, R. A. *J. Electroanal. Chem.* **2002**, *524*−*525*, 242.

(34) Clavilier, J.; Armand, D.; Sun, S. G.; Petit, M. *J. Electroanal. Chem.* **1986**, *205*, 267.

(35) Marković, N. M.; Grgur, B. N.; Lucas, C. A.; Ross, P. N. *Surf. Sci.* **1997**, *384*, L805.

(36) Gómez, R.; Climent, V.; Feliu, J. M.; Weaver, M. J. *J. Phys. Chem.* **2000**, *104*, 597.

(37) Feliu, J. M.; Orts, J. M.; Gómez, R.; Aldaz A.; Clavilier, J. *J. Electroanal. Chem.* **1994**, *372*, 265.

(38) Gómez, R.; Feliu, J. M.; Aldaz, A.; Weaver, M. J. *Surf. Sci.* **1998**, *410*, 48.

(39) This figure was produced using BALSAC program, copyright K. Hermann 1991−9, http://w3.rz-berlin.mpg.de/∼hermann/hermann/balpam.html.

(40) Herrero, E.; Orts, J. M.; Aldaz, A.; Feliu, J. M. *Surf. Sci.* **1999**, *440*, 259.

(41) (a) Smoluchowski, R. *Phys. Rev.* **1941**, *60*, 661. (b) Wandelt, K. *Appl. Surf. Sci.* **1997**, *111*, 1.

(42) Clavilier, J.; El Achi, K.; Rodes, A. *Chem. Phys.* **1990**, *141*, 1.

(43) Clavilier, J.; El Achi, K.; Rodes, A. *J. Electroanal. Chem.* **1989**, *272*, 253.

(44) Gómez, R.; Clavilier, J. *J. Electroanal. Chem.* **1993**, *354*, 189.

(45) Kibler, L. A.; Cuesta, A.; Kleinert, M.; Kolb, D. M. *J. Electroanal. Chem.* **2000**, *484*, 73.

(46) Rodes, A.; Clavilier, J. *J. Electroanal. Chem.* **1993**, *344*, 269.

(47) Lucas, C. A.; Marković, N. M.; Ross, P. N. *Phys. Rev. Lett.* **1996**, *77*, 4922.

(48) Climent, V.; Gómez, R.; Feliu, J. M. *Electrochim. Acta* **1999**, *45*, 629.

(49) Angerstein-Kozlowska, H.; Conway, B. E.; Sharp, W. B. *J. Electroanal. Chem.* **1973**, *43*, 9.

(50) Reutt-Robey, J. E.; Doren, D. J.; Chabal, Y. J.; Christman, S. B. *Phys. Rev. Lett.* **1988**, *61*, 2778.

(51) Reutt-Robey, J. E.; Chabal, Y. J.; Doren, D. J.; Christman, S. B. *J. Vac. Sci. Technol. A* **1989**, *7*, 2227.

(52) Reutt-Robey, J. E.; Doren, D. J.; Chabal, Y. J.; Christman, S. B. *J. Chem. Phys.* **1990**, *93*, 9113.

(53) Ma, J.; Xiao, X.; DiNardo, N. J.; Loy, M. M. T. *Phys. Rev. B* **1998**, *58*, 4877.

(54) Seebauer, E. G.; Allen, C. E. *Prog. Surf. Sci.* **1995**, *49*, 265.

(55) Lebedeva, N. P.; Rodes, A.; Feliu, J. M.; Koper, M. T. M.; van Santen, R. A., *J. Phys. Chem. B* **2002**, *106*, 9863.

(56) Koper, M. T. M.; Lebedeva, N. P.; Hermse, C. G. M. *Faraday Discuss.* **2002**, *121*, 301.

(57) Chang, S.-C.; Weaver, M. *J. Chem. Phys.* **1990**, *92*, 4582.

(58) Friedrich, K. A.; Geyzers, K.-P.; Marmann, A.; Stimming, U.; Vogel, R. *Z. Phys. Chem.* **1999**, *208*, 137.

(59) Gasteiger, H. A.; Marković, N.; Ross, P. N.; Cairns, E. J. *J. Phys. Chem.* **1994**, *98*, 617.

(60) Wartnaby, C. E.; Stuck, A.; Yeo, Y. Y.; King, D. A. *J. Phys. Chem. B* **1996**, *100*, 12483.

(61) Ertl, G.; Neumann, M.; Streit, K. M. *Surf. Sci.* **1977**, *64*, 411.

(62) Palaikis, L.; Zurawski, D.; Hourani, M.; Wieckowski, A. *Surf. Sci.* **1988**, *199*, 183.

(63) Richarz, F. *Elektrochemisch Erzeugte Pt, Ru und PtRu-Elektroden: Charakterisierung und Elektrooxidation von Kohlenmonoxid*; VDI: Düsseldorf, 1995.

(64) Zhu, Y.; Uchida, H.; Watanabe, M. *Langmuir* **1999**, *15*, 8757.